Macromolecules
ARTICLE

Macromolecules **2010**, *43*, 2897–2903 **2897**
DOI: 10.1021/ma902467k

Simultaneous Increase in Seebeck Coefficient and Conductivity in a Doped Poly(alkylthiophene) Blend with Defined Density of States

J. Sun,[†] M.-L. Yeh,[†] B. J. Jung,[†] B. Zhang,[†] J. Feser,[‡] A. Majumdar,[‡] and H. E. Katz*,[†]

[†]*Department of Materials Science and Engineering, Johns Hopkins University, Baltimore, Maryland 21218, and* [‡]*Department of Mechanical Engineering, University of California, Berkeley, California 94720*

Received November 9, 2009; Revised Manuscript Received February 7, 2010

ABSTRACT: The Seebeck coefficient, a defining parameter for thermoelectric materials, depends on the contributions to conductivity of charge carriers at energies away from the Fermi level. Highly conductive materials tend to exhibit conductivity from carriers close to the Fermi level. In this article, we propose polymer blends in which ground state hole carriers, created by doping a minor additive component, are mainly at an orbital energy set below the hole energy of the major component of the blend. Transport, however, is expected to occur through the major component. This leads to a regime in which hole conductivity and Seebeck coefficient may be increased in parallel. While the absolute conductivity of the composite, and thus ZT, are not particularly high, this work demonstrates a route for designing thermoelectric materials in which increases in Seebeck coefficient and conductivity do not cancel each other.

Introduction

Thermoelectric materials are of interest for a wide range of applications in power generation and refrigeration, such as for deep space energy production, automotive waste-heat recovery,[1] and on-chip and larger scale cooling modules.[1−3] The layout of a generic thermoelectric module is shown in Figure 1. When current is driven through the device, heat can be extracted from a region intended to be cooled, as charge carriers absorb heat and are elevated into higher energy states. Recombination of holes and electrons drifting in response to the heat source allows energy extraction at the bottom of the module in the powering mode.

For near room temperature applications, such as refrigeration and waste heat recovery up to 200 °C, Bi_2Te_3−Sb_2Te_3 alloys with ZT ≈ 1 have been used for both n- and p-type thermoelectric systems.[4] For midtemperature power generation (500−900 K), materials based on group IV tellurides are typically used, such as PbTe, GeTe, or SnTe.[5,6] For the highest-temperatures (> 900 K), thermoelectric generators have typically used Si−Ge alloys for both n- and p-type legs.[3]

The performance of thermoelectric materials is determined by a dimensionless quantity called the figure of merit, ZT, defined by eq 1

$$\mathrm{ZT} = S^2\sigma T/\kappa \quad (1)$$

where S is the Seebeck coefficient (thermoelectric power, the change in voltage per unit temperature difference in a material), σ is the electrical conductivity, T is temperature in kelvin at which the properties were determined (or the average device temperature), and κ is the thermal conductivity. ZT ≈ 1 for several currently used thermoelectric materials[1,7−12] with their efficiency as cooling elements 10−30% of that of compressor refrigerators.[13] ZT in bulk materials has barely doubled even after decades of development.[14] Values of S associated with ZT > 1 materials are on the order of hundreds of μV/K.[15] In metals, S is much lower.

Organic and polymeric semiconductors (OSCs) have been considered as potentially high-ZT materials because of their acknowledged low value of κ, 2−3 orders of magnitude below inorganic semiconductors and metals,[16,17] though the σ/κ ratio may not be particularly high in OSCs. The quantity S in doped OSCs is on the order of tens of μV/K,[18] well below inorganics, though pure (and low-conductivity) organics can have S as high as inorganics.[19] Low values of S in doped organics may be due to unfavorable energy and spatial distribution of the density of states relative to the ground state charge carrier energy. In various theoretical models for S, the increase in number of states with respect to energy at or just above the Fermi level is the major determining factor.[18,20]

Recent progress in the design of OSCs for transistors and solar cells has established high charge carrier mobilities at definite energy levels associated with particular conjugated subunits.[21−24] However, the intentional establishment of a Fermi level with respect to the orbital energies of the molecular components of the high-mobility solids has not yet been reported. Enormous progress has been made in preparing and evaluating OSCs for charge transport. The availability of an increasing library of high mobility OSCs with varied energy levels[25−32] provides a unique opportunity to revisit the field of organic thermoelectrics and to carry out a new design approach.

In this article, we report our initial results on semiconductor blends in which the major component, "bulk" molecular subunits, are designed to have carrier energies just above orbital energies of a minor component "additive". The Fermi level is established by the additive, while the current from injected charge is carried predominantly in the higher energy orbitals of the bulk, as shown in Figure 2. Interestingly, an equimolar "blend", in the form of a hole-stabilizing tetrathiafulvalene side chain on a polyvinylcarbazole, has been reported, though not contemplated for thermoelectricity.[33] The additive is not a dopant; in fact, a dopant could be added as a third component to increase conductivity. According to a recent report, the "doping" could even be supplied via a gate electrode.[34] Doping would not greatly alter the Fermi level, in contrast to previously described systems considered for thermoelectric applications (see below). This situation is effectively equivalent to having a large derivative of density of states with respect to energy. In cooling mode, injected charge transfers energy across a sample. In powering mode, the

*To whom correspondence should be addressed.

Published on Web 02/22/2010

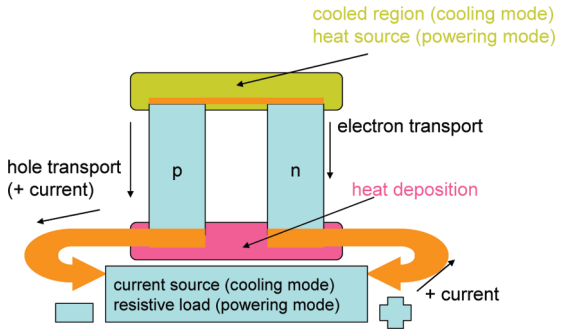

Figure 1. Layout and current paths of a thermoelectric module based on one pn semiconductor couple.

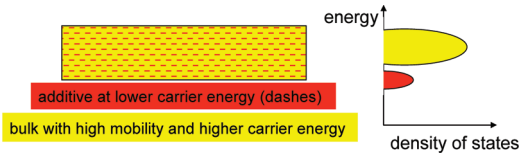

Figure 2. Schematic of proposed organic thermoelectric composite, consisting of an additive that sets the Fermi level and a bulk in which charge carriers at higher energy levels are transported.

thermal excitation of additive-centered charge carriers in one region of the sample will lead to the migration of some of them into the bulk energy levels of another region of the sample, producing a thermovoltaic effect.

The significant new result reported here is that unlike in any previous studies a regime is identified in which Seebeck coefficient and electrical conductivity both increase as a result of doping. This phenomenon is not observed in controls without the additive in which charge carriers are more stable.

Theory of Thermoelectricity. General theoretical principles have been reviewed by Tritt and Subramanian,[15] by DiSalvo,[13] and by Chen and Dresselhaus et al.[11] Thermoelectric cooling occurs when carriers are injected at a certain energy level, usually near a pn junction, and are transported in a higher energy band. The heat flowing away from the injection site, not corrected for heat regeneration, is proportional to the current flowing away from that site (eq 2):

$$Q = \Pi I \tag{2}$$

where Q is heat flow, I is current, and Π is the Peltier coefficient.

However, resistive (I^2R, R = resistance) heating as a result of the current tends to counter the desired cooling, as does thermal conductivity ($\kappa\Delta T$), which leads to reverse heat flow from the heat sink back to the injection site.[1] When charge carriers are the dominant mechanism of heat transfer, such as in many inorganics, a decreased R (lower resistive heating) leads to greater thermal conductivity, and vice versa. In such cases, increasing the current by using more electrically conductive materials is generally counterproductive. However, in low-mobility polymers, thermal conductivity is probably dominated by phonons,[35] so raising electrical conductivity would be helpful. Of course, reducing the resistive heating by lowering the current also lowers the attainable cooling effect in the first place. Thus, there is an optimal current at which the coldest attainable junction temperature is obtained; this temperature is proportional to $\Pi^2/R\kappa$

The quantities Π and S are related by eq 3:

$$\Pi = (S_n - S_p)T \tag{3}$$

where subscripts refer to the different materials at the pn junction and S carries the sign of its dominant carrier and so are generally additive. Because Π^2 is thereby proportional to S^2, and R is inversely proportional to σ, the material figure of merit $ZT = S^2\sigma T/\kappa$ (eq 1) is derived. Cooling efficiency is roughly linear in ZT for $ZT < 1$. Power generation efficiency also increases with ZT, but via a more complicated function of the hot and cold temperatures that is approximately proportional to $(1 + ZT)^{0.5}$ for ZT of about 1 and T of about 350 K.[1,15]

The major factor limiting increases in S is the suboptimal, and in many cases poorly understood, band structure of the semiconductors. Energy levels of organic materials are governed primarily by molecular orbitals, which are more easily estimated than are band structures in inorganics, because the dispersions in the bands are generally lower in organics than in inorganic semiconductors, and relationships between orbital energy levels and molecular structures are well understood from physical organic chemistry. Orbital energies are derivable by combinations of spectroscopy, electrochemistry, and semiempirical calculation. We thus have a considerable degree of control over densities of states in organic solids.

Background on Organic and Polymer Thermoelectrics. Gao has published a numerical model applicable to organic materials.[18,20] The main conclusion is that the Seebeck coefficient S increases as greater proportions of the electrical conductivity occur at energies different from the Fermi level. This in turn depends on the existence of states away from the Fermi level, the probability of their occupancy, and the charge carrier mobility in these states. After showing that the model was applicable to an exemplary inorganic, $CsBi_4Te_6$, the model was successfully used to analyze S for doped poly(3-decylthiophene). Agreement between theory and experiment was achieved despite the possibility that chemical effects other than simple carrier creation could result from the doping and that the band model used to investigate conductivity in inorganics may well not apply to polymers. Gao concluded that an improved material could be obtained if it had localized bands near the Fermi level as well as highly dispersive (high mobility) bands above the Fermi level. A chemical structure was suggested, which while expected to be unstable, gave a theoretically predicted 5-fold increase in S compared to polythiophene. The highly dispersive transport band ranged 0.3 eV above the Fermi level and higher. A different numerical analysis based on percolation of a high conductivity organic component through a low conductivity/high S organic matrix projected an enormous ZT, on the order of 10, if the conducting component has conductivity $> 100\ \Omega^{-1}\ cm^{-1}$ and has a very low percolation threshold.[36,37]

Wuesten et al.[19] considered a similar model but allowed for hopping transport and effects of defects typical of organics, such as grain boundaries, that produce additional localized states. Conductivity versus temperature follows stretched forms of $\exp(-E_H/kT)$, where E_H is the activation energy for hopping. Both the Gao and Wuesten models predict the experimental observation that high doping levels decrease S because the Fermi level is brought closer and closer to the energy level where charge transport is favored.[38] This behavior has been observed in poly(3-decylthiophene),[18] perylenetetracarboxylic dianhydride (PTCDA),[19] vanadyl and zinc phthalocyanine (VOPc and ZnPc),[39,40] polyaniline and polypyrrole,[38] and poly-(3,6-dihexyl-2,7-carbazolenevinylene) (PCVH).[41] S approaches 1 mV/K in some of the least doped cases but rapidly falls as doping levels approach 20%. The dropoff is greater for ZnPc than for VOPc.[40] PCVH is notable for retaining significant S even at 20% doping. A recent and promising report describes doped carbazole polymers with S of 70 μV/K and with an unusually high electrical conductivity of up to 500 S/cm.[42,43] Table 1 summarizes properties of these materials.

Table 1. Dependence of *S* on Doping Levels in Previous Organic and Polymeric Materials

material	low doping level (mol %)	S (μV/K), $S^2\sigma$ (W/mK^2)	high doping level (mol %)	S (μV/K), $S^2\sigma$ (W/mK^2)
polythiophene	15	13−18, 3.2×10^{-6}	19	5−10 (calcd), 10^{-5}
PTCDA	0	300, 1.2×10^{-9}	40	3, 2.9×10^{-11}
VOPc	0	1200, 1.4×10^{-14}	2, considered "low"	700, 4.9×10^{-11}
polyaniline	(conductivity 10^{-3} Ω^{-1} cm^{-1})	ca. 100, 10^{-9}	(conductivity 10^{2} Ω^{-1} cm^{-1})	0, 0
polypyrrole	(conductivity 10^{-1} Ω^{-1} cm^{-1})	60, 3.6×10^{-8}	(conductivity 10^{2} Ω^{-1} cm^{-1})	5, 2.5×10^{-7}
PCVH	2	600, 4.7×10^{-9}	20	200, 2×10^{-8}
PVK copolymer	30	70, 1.9×10^{-5}	100	15, 7.5×10^{-6}

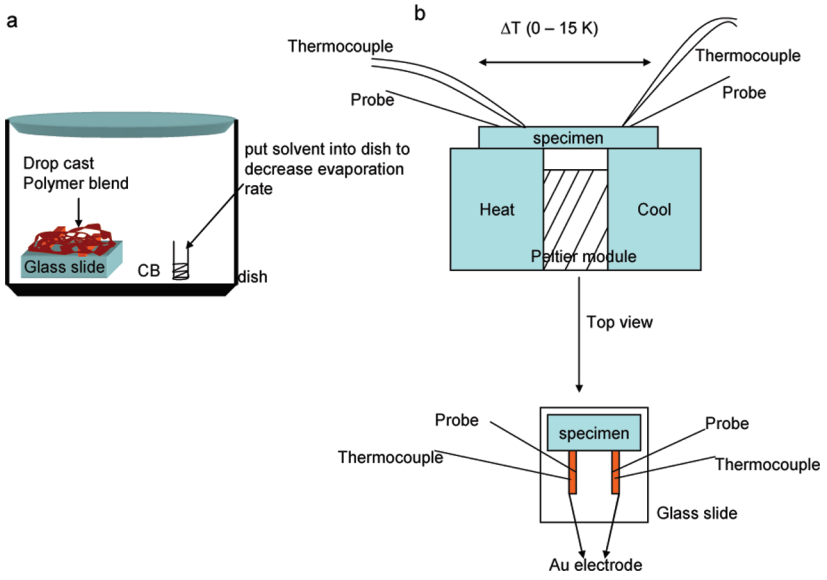

Figure 3

While all of these organic materials were studied as mixtures with dopants, in none of these cases were additional compounds introduced to alter the level at which charge carriers were induced by the dopants, and no effort was made to control or maximize charge carrier mobility above the Fermi level as dopants were added. *This paper represents a first attempt to engineer OSCs with these goals in mind.*

Experimental Section

Materials. Poly(3-hexylthiophene) (P3HT) was purchased from Rieke Metals Inc. and purified by the Soxhlet extraction[44] with methanol, hexane, ethyl acetate, and dichloromethane. Its conductivity as a nominally "neat" film was in the range of 10^{-7}−10^{-6} S/cm.[45] Poly(3-hexylthiothiophene) (P3HTT) was purchased from Rieke Metals Inc. and used as received. Tetrafluorotetracyanoquinodimethane (F_4TCNQ) was purchased from Aldrich and used as received. Cytop, a hydrophobic polyperfluoroalkenyl vinyl ether, was purchased from Asahi Glass Co.

Sample Fabrication. P3HT, P3HTT and F4TCNQ were each separately dissolved in chlorobenzene at appropriate concentrations, and then different ratios of them were mixed together and drop-cast on glass substrate with prepatterned gold electrodes (8 mm in width, 2.5 mm in length, ca. 100 nm thickness by vapor deposition). Films were slowly dried in a dish at room temperature for 2 days (Figure 3a). The morphology and thickness of the cast films were acquired by AFM. Roughness assayed by AFM was around 100 nm (Figure 4), indicating that the films were reasonably continuous, with thickness varying from the average by 10−15% in different regions.

Electrical and Thermoelectric Characterization. Cyclic voltammetry was performed on P3HT and P3HTT versus ferrocene internal standard in 0.1 M tetrabutylammonium PF_6 in acetonitrile. The experiment was performed under nitrogen flow

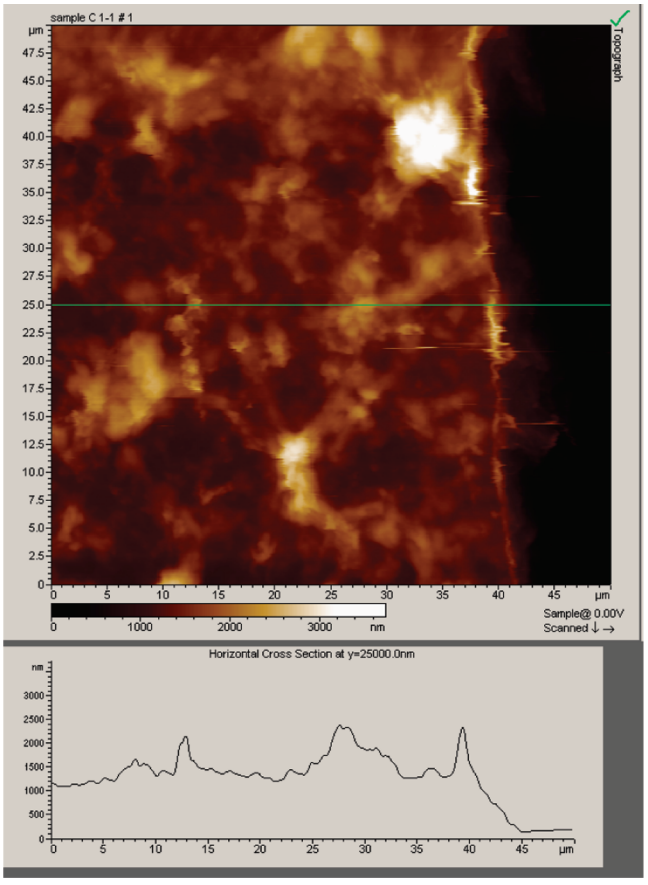

Figure 4. AFM image of drop-cast blend polymer on Si substrate.

Table 2

sample	P3HT, μL (10 mg/mL)	P3HTT (N/A)	F4TCNQ, μL (0.5 mg/mL)	power factor ($W\ m^{-1}\ K^{-2}$)	ZT (κ = 0.17−0.48 W/mK)	film thickness (cm)
A	200	N/A	10	5.966×10^{-9}	3.7×10^{-6}−1.1×10^{-5}	1.75×10^{-4}
C	200	N/A	30	5.085×10^{-9}	3.2×10^{-6}−8.91×10^{-6}	1.75×10^{-4}
D	200	N/A	40	5.07×10^{-9}	3.14×10^{-6}−8.89×10^{-6}	1.75×10^{-4}
F	200	N/A	60	4.876×10^{-9}	3.03×10^{-6}−8.55×10^{-6}	1.75×10^{-4}
G	200	N/A	70	4.965×10^{-9}	3.08×10^{-6}−8.70×10^{-6}	1.75×10^{-4}
H	200	N/A	80	6.053×10^{-9}	3.75×10^{-6}−1.06×10^{-5}	1.75×10^{-4}

Table 3

sample	P3HT, μL (10 mg/mL)	P3HTT, μL (1 mg/mL)	F4TCNQ, μL (0.5 mg/mL)	power factor ($W\ m^{-1}\ K^{-2}$)	ZT (κ = 0.17−0.48 W/mK)	film thickness (cm)
A	200	40	10	7.23×10^{-9}	4.49×10^{-6}−1.27×10^{-5}	2.25×10^{-4}
B	200	40	20	7.26×10^{-9}	4.50×10^{-6}−1.27×10^{-5}	2.25×10^{-4}
C	200	40	30	6.25×10^{-9}	3.88×10^{-6}−1.10×10^{-5}	2.25×10^{-4}
D	200	40	40	7.58×10^{-9}	4.71×10^{-6}−1.33×10^{-5}	2.25×10^{-4}
E	200	40	50	1.16×10^{-9}	7.2×10^{-6}−2.03×10^{-5}	2.25×10^{-4}
F	200	40	60	3.71×10^{-9}	2.31×10^{-6}−6.51×10^{-6}	2.25×10^{-4}

Table 4

sample	P3HT, μL (10 mg/mL)	P3HTT, μL (4 mg/mL)	F4TCNQ, μL (0.5 mg/mL)	power factor ($W\ m^{-1}\ K^{-2}$)	ZT (κ = 0.17−0.48 W/mK)	thickness (cm)
A	200	40	10	4.62×10^{-10}	2.87×10^{-7}−8.09×10^{-7}	2.5×10^{-4}
B	200	40	20	6.83×10^{-10}	4.24×10^{-7}−1.20×10^{-6}	2.5×10^{-4}
C	200	40	30	9.55×10^{-10}	5.93×10^{-7}−1.67×10^{-6}	2.5×10^{-4}
E	200	40	50	1.12×10^{-9}	6.95×10^{-7}−1.96×10^{-6}	2.5×10^{-4}
F	200	40	60	1.33×10^{-9}	8.26×10^{-7}−2.34×10^{-6}	2.5×10^{-4}
G	200	40	70	1.19×10^{-9}	7.39×10^{-7}−2.08×10^{-6}	2.5×10^{-4}
H	200	40	80	1.26×10^{-9}	7.87×10^{-7}−2.21×10^{-6}	2.5×10^{-4}
I	200	40	90	1.02×10^{-9}	6.33×10^{-7}−1.79×10^{-6}	2.5×10^{-4}

Table 5

sample	P3HT, μL (10 mg/mL)	P3HTT, μL (10 mg/mL)	F4TCNQ, μL (0.5 mg/mL)	power factor ($W\ m^{-1}\ K^{-2}$)	ZT (κ = 0.17−0.48 W/mK	thickness (cm)
A	200	40	10	1.09×10^{-9}	6.77×10^{-7}−1.62×10^{-6}	3.10×10^{-4}
B	200	40	20	1.66×10^{-9}	1.03×10^{-6}−2.47×10^{-6}	3.10×10^{-4}
C	200	40	30	2.58×10^{-9}	1.60×10^{-6}−3.85×10^{-6}	3.10×10^{-4}
D	200	40	40	3.99×10^{-9}	2.47×10^{-6}−5.95×10^{-6}	3.10×10^{-4}
F	200	40	60	4.82×10^{-9}	2.99×10^{-6}−7.18×10^{-6}	3.10×10^{-4}
G	200	40	70	2.17×10^{-9}	1.35×10^{-6}−3.24×10^{-6}	3.10×10^{-4}
H	200	40	80	4.78×10^{-9}	2.97×10^{-6}−7.12×10^{-6}	3.10×10^{-4}

after a 10-minute nitrogen purge. The reduction potential of F4TCNQ is approximately 0.1−0.2 V more positive than the polymers,[46] and F4TCNQ is therefore considered to be a strong dopant in the blends studied here. Conductance was measured by obtaining $I-V$ curves on a semiconductor parameter analyzer. The Seebeck coefficient (S) was measured by mounting a sample on a thermoelectric heater−cooler pair, with one electrode of the sample over each. Thermal electromotive force (ΔV) and temperature difference (ΔT) were measured simultaneously by probing the pair of electrodes with a source meter and thermometer and feeding the data into a computer (Figure 3b). Numerous measurements of ΔV, at least 20 and typically 50, were made for each value of ΔT, with a standard deviation of 1−5% (0.01−0.05 mV) per data set. These ΔV are averaged to eliminate the noise signal induced by the environment. Several temperature differences (ΔT) are imposed on the sample. The slopes of plots of averaged ΔV vs ΔT gave values of S. The linearity of the data of ΔV and ΔT is used as a key indicator of valid measurements. In our work, the coefficient of determination, R^2 is invariably above 0.99. Copper wire is used for voltage leads and has very small Seebeck coefficient (1.94 μV/K) as compared to our samples; therefore, the thermoelectric effect from the voltage leads can be neglected. Seebeck measurement is not very sensitive to the film quality as long as there are no cracks or defects destroying the continuity of the film. The Seebeck coefficient measurement was also calibrated by a pure Ni metal sample that is widely utilized as a standard sample for calibrating Seebeck measurements. A very good agreement between our result (-21.4 ± 0.42 μV/K) and reported values (−19.5 and −20.5 μV/K) demonstrates the accuracy of our Seebeck coefficient data. Since four probes are not applied for film conductivity measurements, the contact resistance between Au and P3HT film might have been an issue. Lei et al. already systematically observed the contact resistance between Au and P3HT film by EFM and demonstrated the existence of a high-resistance region in the P3HT close to the Au-on-P3HT contact, whereas the P3HT-on-Au contact exhibits good Ohmic behavior.[47] Our device was fabricated according to P3HT-on-Au configuration, so the contact resistance between them should be minimal.

Thermal conductivity was measured using the 3-omega method[48] on a sample of highly F4TCNQ-doped P3HT (sample prepared as in Table 5 sample H, conductivity is $\sim 1.4 \times 10^{-3}$ S/cm), 1.9 μm on a Si substrate with Cytop fluorinated polymer spin-coated as a 9% solution in perfluorodecalin (2000 rpm, 60 s, thickness around 900 nm). A bare Si substrate with Cytop spin-coated the same way was used as a control sample. Heater lines were made by vapor deposition of 250 nm Au on top of the Cytop through a shadow mask.

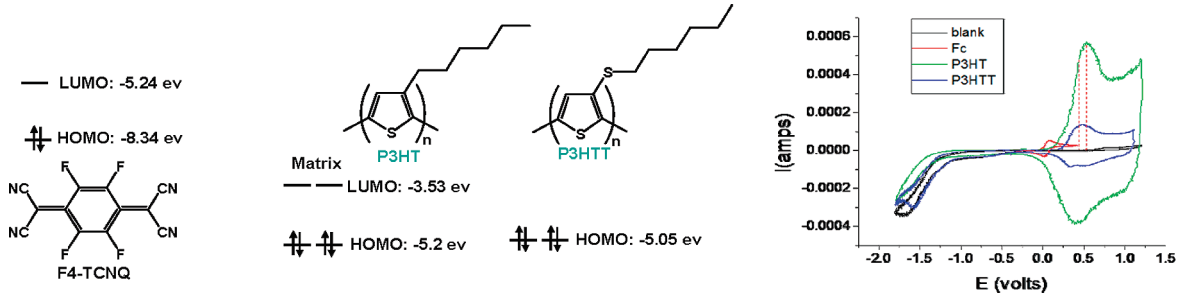

Figure 5. Molecular structures, orbital energies, and CV measurements of P3HT and P3HTT. The structure and energies for F4-TCNQ are also shown. The oxidation peak for P3HTT is 0.15 V less positive than for P3HT, indicating a lower hole energy; the difference is indicated by the dotted red lines. Assignments of absolute energy values are based on P3HT at 5.2 eV.[49]

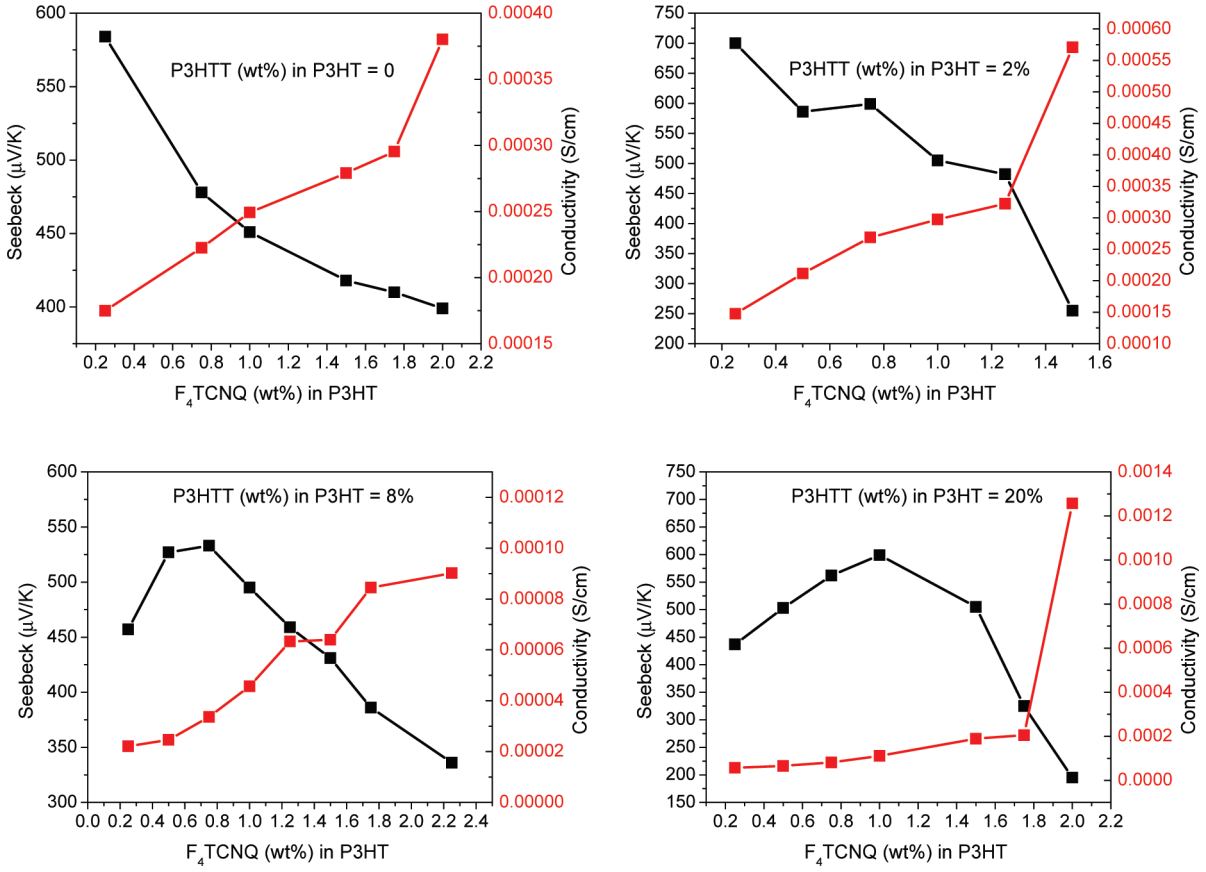

Figure 6. Plots of S and conductivity versus sample number for each data set, 1−4, top left, top right, bottom left, bottom right, respectively.

Results

Electrochemistry of P3HT and P3HTT. Figure 5 shows overlaid oxidation and reduction waves for P3HT and P3HTT. The peak currents for both scanning directions are ca. 0.15 V more positive for P3HT, indicating that, as expected, the hole energy for P3HT is slightly higher than for P3HTT. The energy distributions for each polymer should be somewhat broadened in a blend due to interchain interactions. Still, in a blend of a small quantity of P3HTT in P3HT, holes should be injected and equilibrated in the P3HTT chains but be promoted into higher energy states on P3HT chains for the most efficient transport.

Seebeck Coefficients and Conductivities. Data from four sets of films are described here. Sets 1−4 are listed in Tables 2−5, respectively. As mentioned above, at least 20 voltages were recorded for any one sample at a given temperature difference. Each Seebeck coefficient is the slope of a plot of those voltages versus temperature difference. There are two particularly notable observations. First, the highest thermopower ($S^2\sigma$) was derived from a polymer blend film (set 2, sample E). Second, for the blends with increased amounts of P3HTT (sets 3 and 4), there are regimes in which Seebeck coefficient and electrical conductivity increase simultaneously. Figure 6 shows plots of these two parameters as a function of doping level for each data set. While the highest thermopower was actually obtained in set 2, the most interesting scientific outcome is the trend of sets 3 and 4. Note that for the first three or four data points in these sets, S and conductivity both increase as doping level increases. The acquisition of data set 3 was repeated in its entirety. The Seebeck coefficients were reproduced to within 20%, as was the trend of simultaneously increasing Seebeck coefficient and electrical conductivity for 0.2%−0.7% F4TCNQ. The absolute electrical conductivity in the repeated experiment was an

order of magnitude higher for all samples because of better quality P3HT. To our knowledge, this is the first report of the maintenance or increase of S as doping is increased. Even for set 2, the blending of the two polymers prevents or diminishes the generally observed decrease in S as dopant is added.

Thermal Conductivity. Six measurements were made on the P3HT sample corresponding to sample H in the first chart above. Values were 0.38, 0.41, 0.59, 0.50, 0.53, and 0.46 W/mK, for an average of 0.48 W/mK. This is only slightly higher than a typical value of 0.17 W/mK for other nonpolar polymers such as polystyrene.[50] Measurements on undoped samples were more erratic. On the basis of both the Wiedemann−Franz projection of the thermal conductivity from the electrical conductivity in disordered conductors[51−53] and an experimental comparison of the electrical and thermal conductivities of poly(pyrrole),[54] the thermal conductivity is most likely independent of doping level in samples considered here and is probably dominated by phonons. It is likely that only when conductivities a few orders of magnitude higher are reached will electron-mediated thermal conductivity become important.

Conclusions

The importance of this work is not in the absolute values of S, thermopowers, or associated ZT. As it happens, the values of S are among the higher ones reported for semiconducting polymers, though the thermopowers are orders of magnitude lower than those reported for previous polymer systems. Rather, this work is meant to demonstrate the principle that organic-based compositions may be designed with intentional density-of-states inhomogeneities, defined by relative molecular orbital energies derived from electrochemistry and relative mass fractions, guided by the theoretically preferred density of states distributions for thermoelectric materials. The demonstration was successful and to our knowledge is the first such system explored.

This initial study is of a single pair of polymers that differ only slightly in oxidation potential, used as a marker for hole energy. Obviously, different mixtures of semiconducting polymers and even small molecules can be considered that have larger differences in oxidation potentials and could even define more precisely tailored density of states profiles through the use of three or more oxidizable species. Of course, electron-carrying semiconductor mixtures can also be used to provide the companion n-semiconductor side of a module. In both cases, controlled doping can define the Fermi level to have an arbitrary offset from the energy level of the principal high-mobility component. There is ultimately a trade-off between introducing thermal activation in the conductivity, which increases S, and having the energy barrier between ground state and conducting charge carriers be so great that conductivity is unlikely, lowering σ. The determination of the optimal activation barrier, and the enhancement of mobility, which would also increase σ and thermopower in these blends, is the goal of our future work.

Acknowledgment. Acknowledgment is made to the donors of the American Chemical Society Petroleum Research Fund for primary support of this research. We also thank DOE office of Basic Energy Sciences (Contract DE-FG02-07ER46465) and the JHU MRSEC for additional funding of this work.

References and Notes

(1) Sharp, J.; Bierschenk, J.; Lyon, H. B. Overview of solid-state thermoelectric refrigerators and possible applications to on-chip thermal management. *Proc. IEEE* **2006**, *94* (8), 1602–1612.
(2) Bell, L. E. Cooling, heating, generating power, and recovering waste heat with thermoelectric systems. *Science* **2008**, *321* (5895), 1457–1461.
(3) Snyder, G. J.; Toberer, E. S. Complex thermoelectric materials. *Nat. Mater.* **2008**, *7* (2), 105–114.
(4) Sales, B. C. Critical overview of recent approaches to improved thermoelectric materials. *Int. J. Appl. Ceram. Technol.* **2007**, *4* (4), 291–296.
(5) Wood, C. Materials for Thermoelectric Energy-Conversion. *Rep. Prog. Phys.* **1988**, *51* (4), 459–539.
(6) Gelbstein, Y.; Dashevsky, Z.; Dariel, M. P. High performance n-type PbTe-based materials for thermoelectric applications. *Physica B: Condens. Matter* **2005**, *363* (1−4), 196–205.
(7) Bottner, H.; Chen, G.; Venkatasubramanian, R. Aspects of thin-film superlattice thermoelectric materials, devices, and applications. *MRS Bull.* **2006**, *31* (3), 211–217.
(8) Ahn, K.; Li, C. P.; Uher, C.; Kanatzidis, M. G. Improvement in the Thermoelectric Figure of Merit by La/Ag Cosubstitution in PbTe. *Chem. Mater.* **2009**, *21* (7), 1361–1367.
(9) Chowdhury, I.; Prasher, R.; Lofgreen, K.; Chrysler, G.; Narasimhan, S.; Mahajan, R.; Koester, D.; Alley, R.; Venkatasubramanian, R. On-chip cooling by superlattice-based thin-film thermoelectrics. *Nat. Nanotechnol.* **2009**, *4* (4), 235–238.
(10) Yan, Q. Y.; Chen, H.; Zhou, W. W.; Hng, H. H.; Boey, F. Y. C.; Ma, J. A Simple Chemical Approach for PbTe Nanowires with Enhanced Thermoelectric Properties. *Chem. Mater.* **2008**, *20* (20), 6298–6300.
(11) Chen, G.; Dresselhaus, M. S.; Dresselhaus, G.; Fleurial, J. P.; Caillat, T. Recent developments in thermoelectric materials. *Int. Mater. Rev.* **2003**, *48* (1), 45–66.
(12) Venkatasubramanian, R.; Siivola, E.; Colpitts, T.; O'Quinn, B. Thin-film thermoelectric devices with high room-temperature figures of merit. *Nature* **2001**, *413* (6856), 597–602.
(13) DiSalvo, F. J. Thermoelectric cooling and power generation. *Science* **1999**, *285* (5428), 703–706.
(14) Majumdar, A. Thermoelectricity in semiconductor nanostructures. *Science* **2004**, *303* (5659), 777–778.
(15) Tritt, T. M.; Subramanian, M. A. Thermoelectric materials, phenomena, and applications: A bird's eye view. *MRS Bull.* **2006**, *31* (3), 188–194.
(16) Lodha, A.; Singh, R. Prospects of manufacturing organic semiconductor-based integrated circuits. *IEEE Trans. Semicond. Manuf.* **2001**, *14* (3), 281–296.
(17) Goodson, K. E.; Ju, Y. S. Heat conduction in novel electronic films. *Annu. Rev. Mater. Sci.* **1999**, *29*, 261–293.
(18) Gao, X.; Uehara, K.; Klug, D. D.; Tse, J. S. Rational design of high-efficiency thermoelectric materials with low band gap conductive polymers. *Comput. Mater. Sci.* **2006**, *36* (1−2), 49–53.
(19) Wuesten, J.; Ziegler, C.; Ertl, T. Electron transport in pristine and alkali metal doped perylene-3,4,9,10-tetracarboxylicdianhydride (PTCDA) thin films. *Phys. Rev. B* **2006**, *74* (12).
(20) Gao, X.; Uehara, K.; Klug, D. D.; Patchkovskii, S.; Tse, J. S.; Tritt, T. M. Theoretical studies on the thermopower of semiconductors and low-band-gap crystalline polymers. *Phys. Rev. B* **2005**, *72* (12).
(21) Dobabalapur, A.; Katz, H. E.; Torsi, L. Molecular orbital energy level engineering in organic translators. *Adv. Mater.* **1996**, *8* (10), 853.
(22) Hong, X. M.; Katz, H. E.; Lovinger, A. J.; Wang, B. C.; Raghavachari, K. Thiophene-phenylene and thiophene-thiazole oligomeric semiconductors with high field-effect transistor on/off ratios. *Chem. Mater.* **2001**, *13* (12), 4686–4691.
(23) Laquindanum, J. G.; Katz, H. E.; Lovinger, A. J. Synthesis, morphology, and field-effect mobility of anthradithiophenes. *J. Am. Chem. Soc.* **1998**, *120* (4), 664–672.
(24) Li, W. J.; Katz, H. E.; Lovinger, A. J.; Laquindanum, J. G. Field-effect transistors based on thiophene hexamer analogues with diminished electron donor strength. *Chem. Mater.* **1999**, *11* (2), 458–465.
(25) Allard, S.; Forster, M.; Souharce, B.; Thiem, H.; Scherf, U. Organic semiconductors for solution-processable field-effect transistors (OFETs). *Angew. Chem., Int. Ed.* **2008**, *47* (22), 4070–4098.
(26) Anthony, J. E.; Heeney, M.; Ong, B. S. Synthetic aspects of organic semiconductors. *MRS Bull.* **2008**, *33* (7), 698–705.
(27) Braga, D.; Horowitz, G. High-Performance Organic Field-Effect Transistors. *Adv. Mater.* **2009**, *21* (14−15), 1473–1486.
(28) de Boer, B.; Facchetti, A. Semiconducting polymeric materials. *Polym. Rev.* **2008**, *48* (3), 423–431.
(29) Di, C. A.; Yu, G.; Liu, Y.; Zhu, D. High-performance organic field-effect transistors: Molecular design, device fabrication, and physical properties. *J. Phys. Chem. B* **2007**, *111* (51), 14083–14096.
(30) Katz, H. E.; Huang, J. Thin-Film Organic Electronic Devices. *Annu. Rev. Mater. Res.* **2009**, *39*, 71–92.

(31) Mas-Torrent, M.; Rovira, C. Novel small molecules for organic field-effect transistors: towards processability and high performance. *Chem. Soc. Rev.* **2008**, *37* (4), 827–838.
(32) McCulloch, I.; Heeney, M.; Chabinyc, M. L.; DeLongchamp, D.; Kline, R. J.; Coelle, M.; Duffy, W.; Fischer, D.; Gundlach, D.; Hamadani, B.; Hamilton, R.; Richter, L.; Salleo, A.; Shkunov, M.; Sporrowe, D.; Tierney, S.; Zhong, W. Semiconducting Thienothiophene Copolymers: Design, Synthesis, Morphology, and Performance in Thin-Film Organic Transistors. *Adv. Mater.* **2009**, *21* (10−11), 1091–1109.
(33) Liu, Y.; Wang, C.; Li, M.; Lai, G.; Shen, Y. Synthesis and spectroscopic and electrochemical properties of TTF-derivatized polycarbazole. *Macromolecules* **2008**, *41* (6), 2045–2048.
(34) Pernstich, K. P.; Rossner, B.; Batlogg, B. Field-effect-modulated Seebeck coefficient in organic semiconductors. *Nat. Mater.* **2008**, *7* (4), 321–325.
(35) Kaul, P. B.; Day, K. A.; Abramson, A. R., Application of the three omega method for the thermal conductivity measurement of polyaniline. *J. Appl. Phys.* **2007**, *101* (8).
(36) Feng, J.; Ellis, T. W. Feasibility study of conjugated polymer nanocomposites for thermoelectrics. *Synth. Met.* **2003**, *135* (1−3), 55–56.
(37) Feng, J.; Ellis, T. W. Thermal management for semiconductor devices with conductive polymers. *Synth. Met.* **2003**, *135* (1−3), 155–156.
(38) Mateeva, N.; Niculescu, H.; Schlenoff, J.; Testardi, L. R. Correlation of Seebeck coefficient and electric conductivity in polyaniline and polypyrrole. *J. Appl. Phys.* **1998**, *83* (6), 3111–3117.
(39) Pfeiffer, M.; Beyer, A.; Fritz, T.; Leo, K. Controlled doping of phthalocyanine layers by cosublimation with acceptor molecules: A systematic Seebeck and conductivity study. *Appl. Phys. Lett.* **1998**, *73* (22), 3202–3204.
(40) Pfeiffer, M.; Beyer, A.; Plonnigs, B.; Nollau, A.; Fritz, T.; Leo, K.; Schlettwein, D.; Hiller, S.; Wohrle, D. Controlled p-doping of pigment layers by cosublimation: Basic mechanisms and implications for their use in organic photovoltaic cells. *Sol. Energy Mater. Sol. Cells* **2000**, *63* (1), 83–99.
(41) Levesque, I.; Gao, X.; Klug, D. D.; Tse, J. S.; Ratcliffe, C. I.; Leclerc, M. Highly soluble poly(2,7-carbazolenevinylene) for thermoelectrical applications: From theory to experiment. *React. Funct. Polym.* **2005**, *65* (1−2), 23–36.
(42) Aich, R. B.; Blouin, N.; Bouchard, A.; Leclerc, M. Electrical and Thermoelectric Properties of Poly(2,7-Carbazole) Derivatives. *Chem. Mater.* **2009**, *21* (4), 751–757.
(43) Levesque, I.; Bertrand, P. O.; Blouin, N.; Leclerc, M.; Zecchin, S.; Zotti, G.; Ratcliffe, C. I.; Klug, D. D.; Gao, X.; Gao, F. M.; Tse, J. S. Synthesis and thermoelectric properties of polycarbazole, polyindolocarbazole, and polydiindolocarbazole derivatives. *Chem. Mater.* **2007**, *19* (8), 2128–2138.
(44) Trznadel, M.; Pron, A.; Zagorska, M. Effect of molecular weight on spectroscopic and spectroelectrochemical properties of regioregular poly(3-hexylthiophene). *Macromolecules* **1998**, *31* (15), 5051–5058.
(45) Chen, T. A.; Wu, X. M.; Rieke, R. D. Regiocontrolled Synthesis of Poly(3-Alkylthiophenes) Mediated by Rieke Zinc - Their Characterization and Solid-State Properties. *J. Am. Chem. Soc.* **1995**, *117* (1), 233–244.
(46) Ferraro, J. R.; Williams, J. M. *Introduction to Synthetic Electrical Conductors*; Academic Press: New York, 1987.
(47) Lei, C. H.; Das, A.; Elliott, M.; Macdonald, J. E.; Turner, M. L. Au-poly(3-hexylthiophene) contact behaviour at high resolution. *Synth. Met.* **2004**, *145* (2−3), 217–220.
(48) Tong, T.; A., M. Re-examining the 3-Omega Technique for Thin Film Thermal Characterization. *Rev. Sci. Instrum.* **2006**, *77*, 104902.
(49) Al-Ibrahim, M.; Roth, H. K.; Zhokhavets, U.; Gobsch, G.; Sensfuss, S. Flexible large area polymer solar cells based on poly-(3-hexylthiophene)/fullerene. *Sol. Energy Mater. Sol. Cells* **2005**, *85* (1), 13–20.
(50) Marcus, S. M.; Blaine, R. L. Thermal Conductivity of Polymers, Glasses, and Ceramics by Modulated DSC. *Thermochim. Acta* **1994**, TA–086.
(51) Guckelsberger, K.; Rodhammer, P.; Gmelin, E.; Peo, M.; Menke, K.; Hocker, J.; Roth, S.; Dransfeld, K. Anomalous Thermal Conductivity of Polyacetylene. *Z. Phys. B: Condens. Matter* **1981**, *43* (3), 189–191.
(52) Kaiser, A. B. Electron-phonon Enhancement of Thermopower--Application to Metallic Glasses. *Phys. Rev. B* **1984**, *29* (12), 7088–7091.
(53) Moses, D.; Denenstein, A. Experimental-determination of the Thermal-conductivity of a Conducting Polymer--Pure and Heavily Doped Polyacetylene. *Phys. Rev. B* **1984**, *30* (4), 2090–2097.
(54) Lunn, B. A.; Unsworth, J.; Booth, N. G.; Innis, P. C. Determination of the Thermal Conductivity of Polypyrrole over the Temperature Range 280−335 K. *J. Mater. Sci.* **1993**, *28*, 5092–5098.